J Solid State Electrochem (2011) 15:1987–1995
DOI 10.1007/s10008-010-1219-1

ORIGINAL PAPER

The effect of solid electrolyte interface formation conditions on the aging performance of Li-ion cells

Chenghuan Huang · Kelong Huang · Haiyan Wang · Suqin Liu · Yuqun Zeng

Received: 25 August 2010 / Revised: 30 September 2010 / Accepted: 10 October 2010 / Published online: 28 October 2010

Abstract The effect of formation temperatures and current densities on the aging performance of $LiNi_{1/3}Co_{1/3}Mn_{1/3}O_2$/artificial graphite Li-ion cells during storage and cycle was investigated using three-electrode electrochemical impedance spectroscopy and charge–discharge experiment. The higher formation temperature at 45 °C decreased the resistance of solid electrolyte interphase (SEI) film and the irreversible capacity loss of Li-ion cells during SEI formation process. After Li-ion cell storage at 60 °C for 10 weeks, the ohmic resistance of the negative electrodes and the irreversible capacity loss of the cells reduced 24% and 7.9%, respectively, accompanied by a significant decrease of SEI film resistance when the formation temperature increased from 25 to 45 °C. The higher temperature at 45 °C may facilitate the transformation of metastable $ROCO_2Li$ to stable inorganics to form a stable SEI film. Three hundred cycling tests indicated that the capacity retention of the cell formation at 25 °C was only 87.5%, about 8% less than that of the cell formation at 45 °C. However, the SEI formation current density did not significantly affect the property of SEI film and the irreversible capacity loss of the aged cells.

Keywords Formation condition · SEI film · Li-ion cell · Aging performance · Capacity loss · Impedance

C. Huang · K. Huang (✉) · H. Wang · S. Liu
School of Chemistry and Chemical Engineering,
Central South University,
Changsha 410083, China
e-mail: huangkelong@yahoo.com.cn

Y. Zeng
Amperex Technology Limited,
Dongguan 523808, China

Introduction

It is generally known that during the initial intercalation of lithium into the graphite negative electrode, the intercalated lithium reacts immediately with the electrolyte components, i.e., the solvents and the salts, forming a passivating layer called solid electrolyte interphase (SEI) [1–5], which is a key component in Li-ion batteries. The performance of Li-ion batteries, such as cyclability, safety, and shelf life, is strongly affected by the nature of the SEI film [1, 6–13]. For example, a thin and compact SEI film with good Li-ion conductivity can enhance the initial capacity and prolong the cycle life of a battery. And a stable SEI film can reduce the capacity fade of a battery when it is used or stored at elevated temperatures. It is known that the self-discharge rate of a battery is mainly governed by the SEI film, and the self-discharge occurs in two main ways, i.e., the de-intercalation and diffusion into the electrolyte of the intercalated lithium ions, and the dissolution and rebuilding of SEI film [9, 14].

Many research works [15–18] have been conducted on the self-discharge of Li-ion cells at various temperatures because storage performance is a crucial factor for Li-ion battery applications. It is found that elevated temperatures accelerate the capacity loss due to the instability of SEI film [16, 18, 19]. Therefore, it is required for the graphite electrode to develop a stable SEI film during its formation step to retard the aging/degradation of a Li-ion battery in high-temperature applications.

However, there is little information about the effect of SEI formation conditions on the characteristics of the SEI layer and especially on the performance of Li-ion batteries in open literatures. Pyun et al. [20, 21] reported that the SEI formation temperature significantly affected the structural and compositional changes of the SEI layer

formed on the graphite electrode in a half cell and showed that the rising formation temperature decreased the resistance to the lithium transport through the SEI layer. Doll et al. [22] claimed that the formation current density also influenced both nature and thickness of the SEI film formed on the graphite electrode in a half cell. But there is no further study on the long-term performance of those half cells with different formation conditions. Furthermore, a half cell contains two "anode-type" electrodes, on both of which an SEI film can be formed [5, 23] because lithiated graphite and metallic lithium have very close potentials. Thus, the aging behavior of a half cell will differ from that of a full cell. In this work, we studied the effect of SEI formation temperatures and current densities on the aging performance of Li-ion cells containing $LiNi_{1/3}Co_{1/3}Mn_{1/3}O_2$ and graphite as the positive and negative electrodes, respectively, and on the characteristics of the SEI film on the graphite electrodes using three-electrode electrochemical impedance spectroscopy (EIS).

Experimental

A series of pouch Li-ion cells with the dimension of 7.6×30×40 mm ($T \times W \times L$) and with the capacity of about 850 mAh contained commercial $LiNi_{1/3}Co_{1/3}Mn_{1/3}O_2$ (ATL supplied, $D_{50} \approx 11$ μm) and artificial graphite (Shanshan, China, $D_{50} \approx 11$ μm) as the active materials, with poly(vinylidene fluoride) as the binder of electrodes, Celgard membrane as the separator, and 1 M $LiPF_6$/ethylene carbonate–propylene carbonate–diethyl carbonate (EC–DEC–PC) as the electrolyte. The cell balance (the capacity ratio of the anode to the cathode) was 1.20. The Li-ion cells with copper and aluminum foils as the current collectors of the negative and positive electrodes, respectively, were spirally wound. All fresh cells were first charged to 3.75 V under different constant currents and followed by a constant voltage charge at 3.75 V until reaching a cutoff current of 16 mA (~0.019 C). This period is conventionally called the formation process. According to different formation conditions, Li-ion cells were divided into three groups, as shown in Table 1. After formation, the cells were degassed and subjected to a few charge–discharge cycles at room temperature in the voltage region from 3.00 to 4.20 V before further study.

Table 1 Three different formation processes

Group	Formation condition		
	Temperature (°C)	Charge current (mA)	Current density ($mA\,cm^{-2}$)
A	45	16	0.043
B	45	400	1.077
C	25	16	0.043

Three groups of cells with 100% state of charge, which had been charged to 4.20 V at a constant current of 80 mA (~0.094 C) and potentiostatic charge at 4.20 V until a cutoff current of 16 mA, were kept in storage at 60 °C for up to 10 weeks. An EIS was performed on these cells before and during storage by a Zahner IM6e electrochemical workstation, with a 5-mV ac perturbation over the frequency range from 20 mHz to 100 kHz at ambient condition. In order to separate the impedance contribution of the positive and negative electrodes to the whole cell, the cells were fabricated with reference microelectrodes, made by tiny copper wires. The naked copper tip being inserted between the negative and positive electrodes was plating Li with a constant current charge at 10 μA before the formation process using Land® charge–discharge instrument (China). The potential of positive electrode is shown in Fig. 1 during plating. The voltage of the positive electrode was stable at 3.44 V after the microelectrode had been plating Li for 10 min. After storage for 10 weeks, the aged cells were discharged at a constant current of 80 mA to 3.00 V to determine their capacity loss.

Cycling tests of Li-ion cells with different formation conditions were performed on Arbin BT-2000 battery tester at ambient condition. The charge–discharge protocol included a constant current charge at 800 mA until the voltage reached 4.20 V, followed by a constant voltage charge at 4.20 V until a cutoff current of 16 mA and a constant current discharge at 800 mA until a cutoff voltage of 3.00 V.

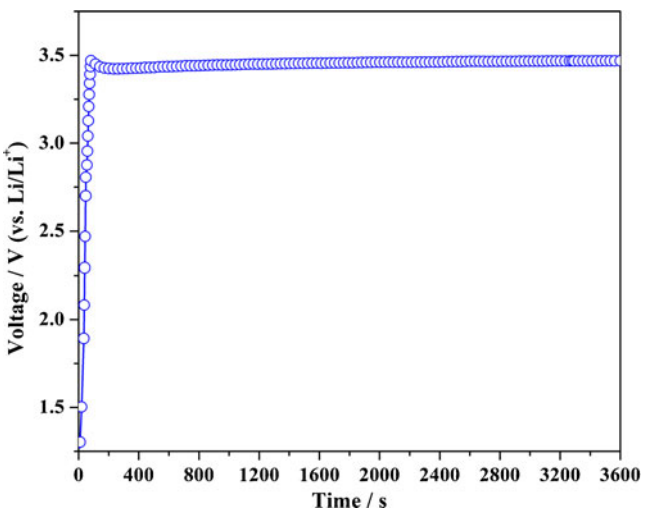

Fig. 1 Voltage profile of the positive electrode vs. reference microelectrode during Li plating onto the microelectrode

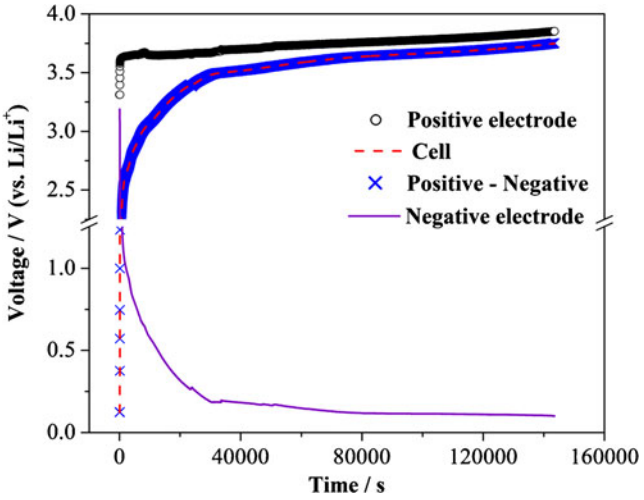

Fig. 2 Voltage profiles of the Li-ion cell (group C) during the formation process

Results and discussion

SEI formation

Figure 2 shows both potential curves of the positive and the negative electrodes in group C during the formation period. The potential difference between the positive electrode and the negative electrode was identical to the voltage of the full cell, indicating that the microelectrode could be used as the reference electrode.

Figure 3 shows the impedance spectra of the graphite electrodes in the Li-ion cells after formation. The cells were first charged to 3.75 V under different formation conditions, followed by the EIS measurements. The impedance spectra consist of an inductive tail at the higher frequency, two separated arcs in the high- and intermediate-frequency range, and an inclined line in the low-frequency range.

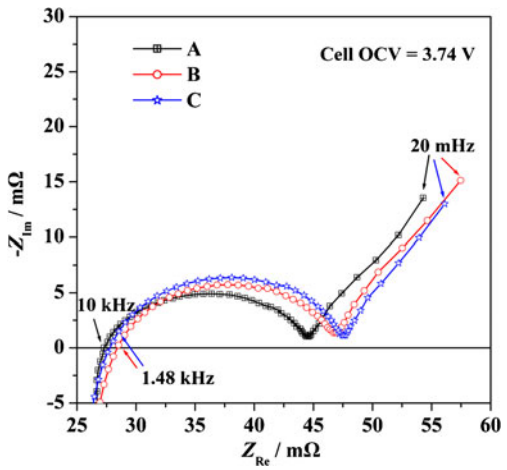

Fig. 3 Impedance spectra of negative electrodes for Li-ion cells after formation at different conditions

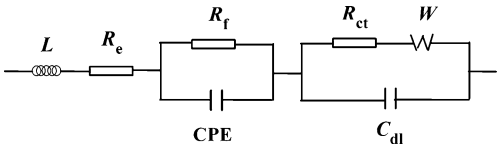

Fig. 4 Equivalent circuit of the negative electrode

The high-frequency arc is due to the impedance for lithium transport through the SEI film formed at different SEI formation conditions; thus, it gives information on the SEI layer property itself [20]. The intermediate-frequency arc is associated with the charge-transfer process at the SEI layer/electrolyte interface [24]. The inclined line at the lower frequency is attributed to the Warburg impedance associated with Li-ion diffusion in the graphite electrode.

To compare the SEI film resistance among the cells with different formation conditions, the equivalent circuit, including the components of the electrolyte and electrodes resistance (R_e), the SEI film resistance (R_f), and the charge-transfer resistance (R_{ct}), was used to fit the impedance spectra, as presented in Fig. 4, where L represents the inductance and W refers to the Warburg resistance. CPE is the corresponding imperfect capacitance to R_f. C_{dl} is the double-layer capacitance. The combination of R_{ct} and W is called faradic impedance, which reflects kinetics of the cell reactions. Low R_{ct} generally corresponds to a fast kinetics of the faradic reaction [25]. The simulation results of R_f and R_{ct}, both of which represent the interfacial resistance, are shown in Fig. 5, indicating that R_f, R_{ct}, and the interfacial resistance on the negative electrode of group A were the smallest. Thus, under the same formation current density of 0.043 mA cm^{-2}, the resistance to the lithium ion transport through the SEI layer deceased when the SEI formation temperature increased from 25 to 45 °C. A similar trend was observed in Fig. 3 of [20] in which the size of the high-frequency arc in the impedance spectrum of graphite electrode was decreased when the SEI formation tempera-

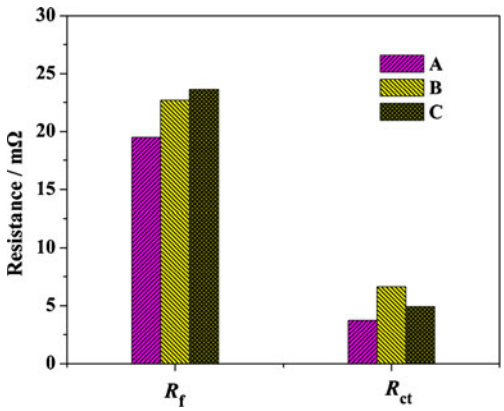

Fig. 5 SEI film resistances and charge-transfer resistances of negative electrodes for Li-ion cells after formation at different conditions

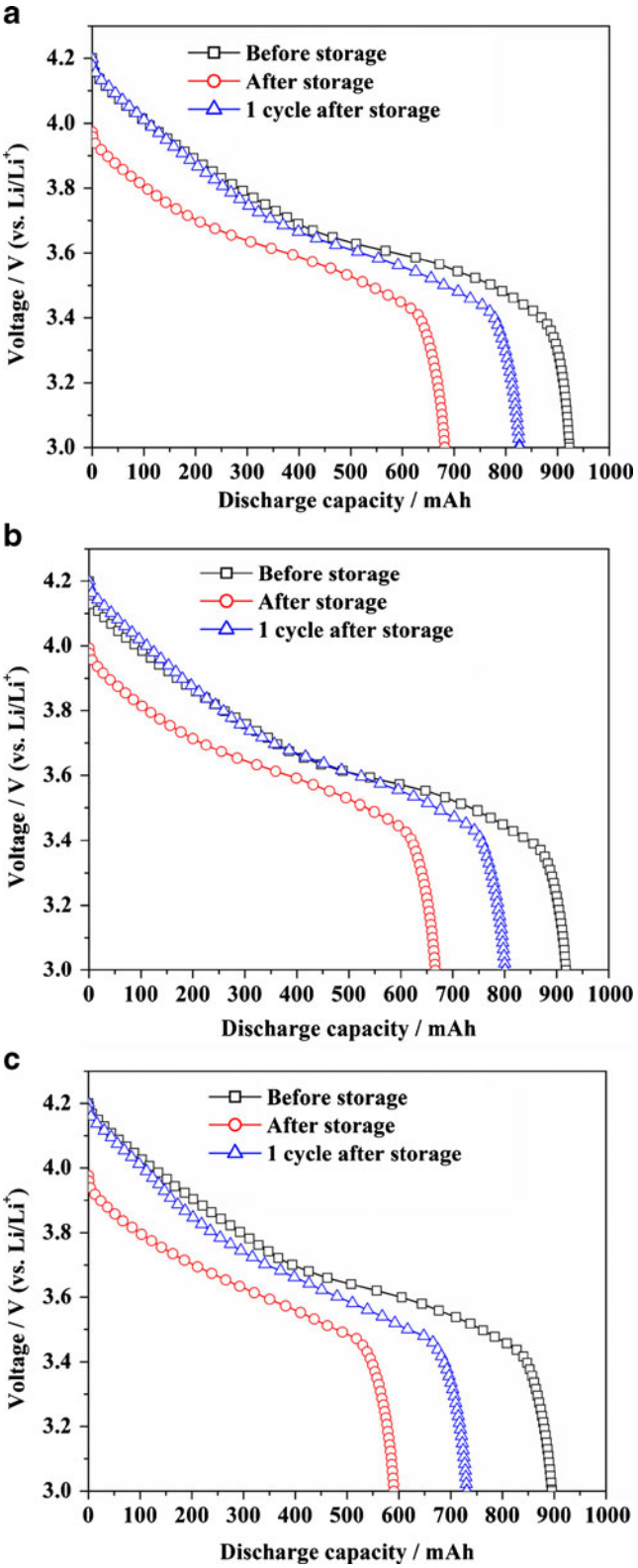

Fig. 6 Discharge capacity of the Li-ion cells with group A (**a**), group B (**b**), and group C (**c**) before and after storage at 60 °C for 10 weeks

ture increased from 0 to 40 °C, inferring that the R_f decreased with rising SEI formation temperature. On the other hand, the higher formation current density at 1.077 mA cm^{-2} increased the resistance of the SEI layer at the formation temperature of 45 °C. Assumed that the specific conductivity of SEI film among these Li-ion cells is the same, the thickness of SEI film of group A will be the smallest, according to:

$$R = \frac{1}{\sigma}\frac{L}{S} \tag{1}$$

where σ is the conductivity, L is the thickness of SEI film, and S is the interface area. The SEI thickness (L) can be expressed as:

$$L = L_0 + kN_L \tag{2}$$

where L_0 is the initial SEI thickness before formation (L_0=0), k is an empirical parameter independent of both time and temperature, and N_L is the number of moles of lithium being reacting during formation. This implied that the N_L in group A was minimal. Thus, group A with the minimal number of lost active lithium ions had the smallest irreversible capacity loss during the SEI formation process. This was confirmed by the initial reversible capacity of the cells after formation. The discharge capacity (with the discharge current at 80 mA) of group A, group B, and group C was 923, 918, and 895 mAh, respectively.

Storage performance

Figure 6 shows the discharge capacity curves of the three groups of Li-ion cells before storage, after storage, and one charge–discharge cycle after storage at 60 °C for 10 weeks. All the aged cells suffered the self-discharge capacity loss after storage. The total capacity loss of group A was smaller than that of group B and group C, as shown in Table 2, illustrating that less active lithium ions were consumed in group A than in the other two groups during storage. It is also observed that a partial capacity loss of the aged cells was recovered after one cycle of charge–discharge. Generally, the self-discharge capacity loss can consist of irreversible and

Table 2 Reversible and irreversible capacity loss of Li-ion cells after storage at 60 °C for 10 weeks

Group	Capacity loss (%)	Irreversible capacity loss (%)	Reversible capacity loss (%)
A	26.1	10.5	15.6
B	27.4	12.8	14.6
C	34.0	18.4	15.6

reversible components. The irreversible capacity loss cannot be recovered because the lost active lithium ions (de-intercalated lithium ions) which are consumed to build insoluble components of SEI film cannot re-intercalate into graphite. Typically, an SEI film is composed of stable (Li_2CO_3 and other inorganics) and metastable (lithium-alkyl carbonates) components [1]. Taking EC as an example, it is reduced on the graphite surface to metastable complexes via a two-electron transfer during storage, according to

$$2\delta EC + 2\delta(e^- \cdot Li_g^+) \rightarrow 2\delta(CH_2CH_2OCO_2Li^\bullet)_{metastable} \quad (3)$$

where $(e^- \cdot Li_g^+)$ represents a pair of electron and lithium ion localized in the SEI film resulting from the de-intercalation reaction [26], which can be written as

$$LiC_6 \rightarrow Li_{1-\delta}C_6 + \delta(e^- \cdot Li_g^+) \quad (4)$$

A part of metastable complexes are transformed into alky lithium-alkyl carbonates or insoluble inorganics on the graphite surface during storage:

$$2n(CH_2CH_2OCO_2Li^\bullet)_{metastable} \rightarrow n(CH_2)_2 + n(CH_2OCO_2Li)_2 \quad (5)$$

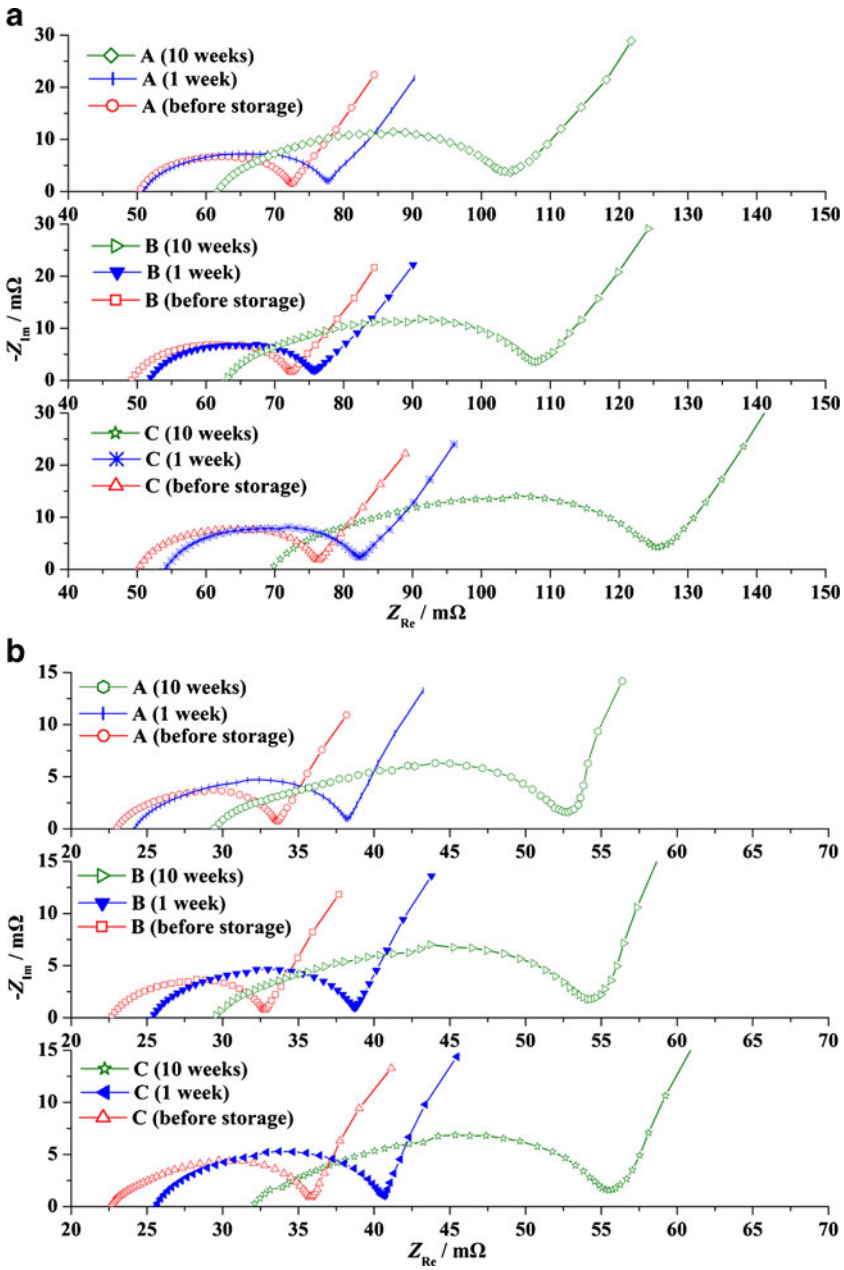

Fig. 7 Nyquist plots of negative electrodes (**a**), positive electrodes (**b**), and full cells (**c**) before and after storage at 60 °C

Fig. 7 (continued)

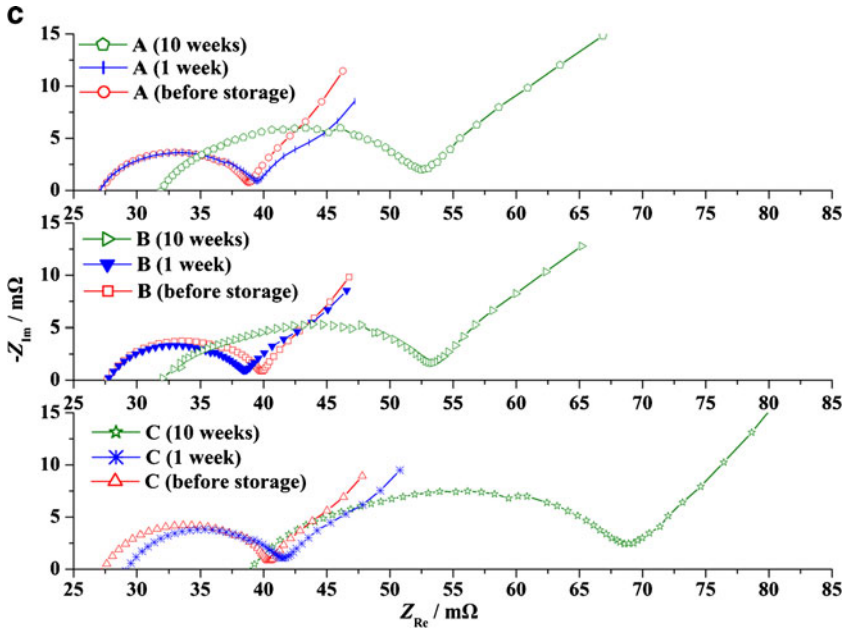

$$2m(CH_2CH_2OCO_2Li^{\bullet})_{metastable} + 2m(e^- \cdot Li_g^+) \rightarrow 2mCH_2CH_2 + 2mLi_2CO_3 \quad (6)$$

Table 2 shows that the irreversible capacity loss of group A was the smallest, with 2.3% and 7.9% less than that of group B and group C, respectively. It is inferred that the smallest amount of insoluble substances was produced in group A during storage. On the other hand, the reversible capacity loss of a cell during storage can be recovered by recharging the cell. Firstly, a portion of metastable complexes of SEI layer dissociates back to the original components upon the recharging step of the cell after storage by the following reaction [26]:

$$2(\delta - n - m)(CH_2CH_2OCO_2Li^{\bullet})_{metastable} \rightarrow 2(\delta - n - m)EC + 2(\delta - n - m)(e^- \cdot Li_g^+) \quad (7)$$

Secondly, during storage at elevated temperatures, some soluble components of the SEI film are partially dissolved, resulting in the liberation of some lithium ions. These liberated ions become active again by recharging the aged cells, and therefore, a partial capacity loss is recovered [16]. Moreover, some liberated lithium ions dissolved in the electrolyte may diffuse to the positive electrode side due to concentration gradient, where the re-intercalation of lithium ions in the $Li_xNi_{1/3}Co_{1/3}Mn_{1/3}O_2$ can occur, resulting in the potential drop of the positive electrode, according to the reaction:

$$Li_xNi_{1/3}Co_{1/3}Mn_{1/3}O_2 + ye^- + yLi^+ \rightarrow Li_{x+y}Ni_{1/3}Co_{1/3}Mn_{1/3}O_2 \quad (8)$$

where electrons are coming from the electrolyte oxidation, occurring in a high voltage range [27]. The superficial oxidation on the positive electrode surface [28] can be written as

$$yEl \rightarrow yEl^+ + ye^- \quad (9)$$

where El is any solvent (EC, PC, or DEC) in the electrolyte. It is found that the reversible capacity loss of the aged cells after storage for 10 weeks was in the range of 14.6–15.6%.

Figure 7 shows the impedance spectra of the three-electrode cells before and after storage at 60 °C. It is found that after 10 weeks, the ohmic resistance rise of the full cell in group C was more than that of the full cells in the other two groups, as shown in Fig. 7a. This rise was mainly contributed by side reactions between the electrodes and the electrolyte. Figure 7b shows that the impedance of all positive electrodes was increasing with the prolonged storage, which was mainly attributed to the superficial oxidation of the electrolyte on the surface of the positive electrode (Eq. 9) and the re-intercalation reaction (Eq. 8) mentioned above. However, compared to the impedance change of the negative electrodes among the three groups of Li-ion cells, that of the positive electrodes was less significant, inferring that the side reactions between the electrodes and the electrolyte were mainly governed by the graphite electrode during storage at 60 °C.

In order to interpret the impedance change of negative electrodes, the equivalent circuit in Fig. 4 was used for modeling of the impedance. The simulation results (in Fig. 8) show the change of different resistances after the cells storage at 60 °C. The ohmic resistance of the negative electrode in group C rapidly increased, followed by group B and then by group A (Fig. 8a). The increase of ohmic resistance was 41.8%, 21.1%, and 17.8% after

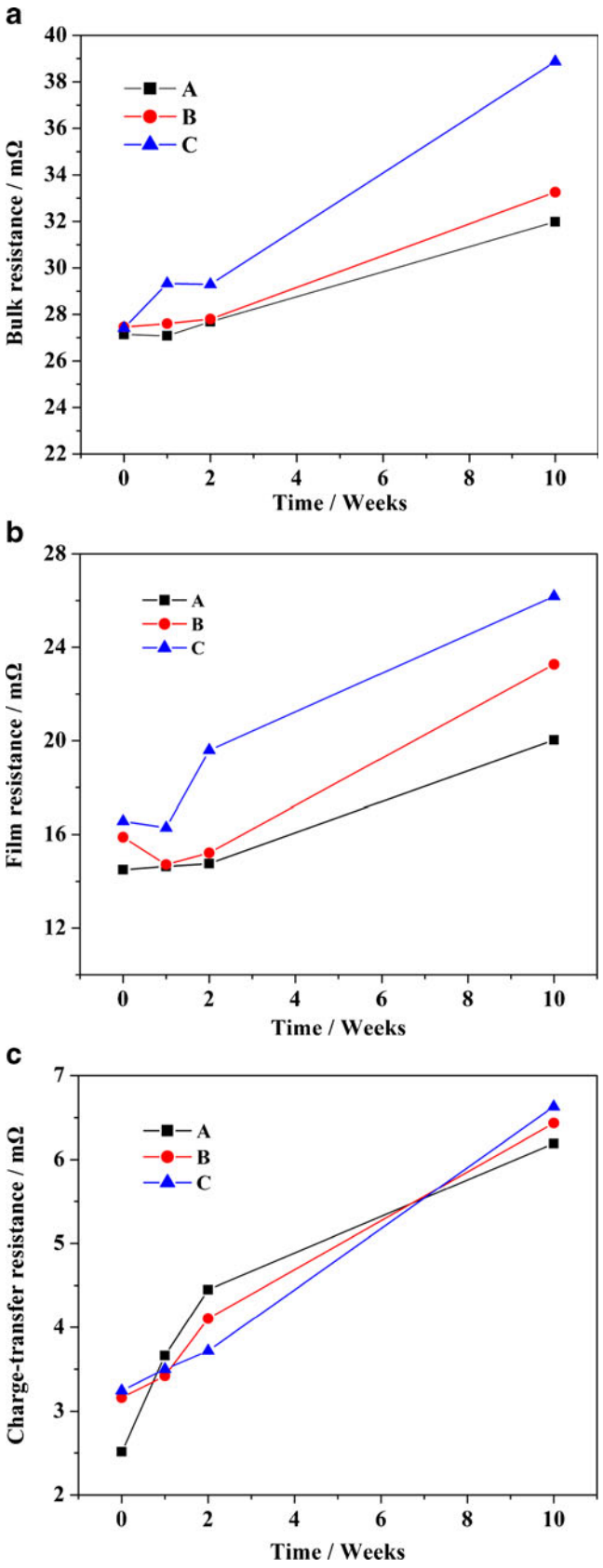

◀ **Fig. 8** Simulation results of ohmic resistances (**a**), SEI film resistances (**b**), and charge-transfer resistances (**c**) of negative electrodes for the Li-ion cells before and after storage at 60 °C

10 weeks for group C, group B, and group A, respectively. Obviously, the side reaction on the graphite electrode of group C was severest, inferring that the SEI film formation at 25 °C was less stable than the formation at 45 °C. In Fig. 8b, c, it reveals that after storage for 10 weeks, both the R_f and R_{ct} of group C were greater than those of the other two groups. The R_f of group C increased 58.0%, about 20% and 17% higher than the increase of SEI film resistances of group A and group B, respectively. Furthermore, it is noted that the R_f of group C decreased at the first week and then increased thereafter, implying that it was not as stable as the SEI film of group A. The R_f of group A slowly increased with the prolonged storage. The unstable SEI film would suffer dissolution at the beginning of the storage at the high temperature. Pyun et al. [20, 21] reported that the higher SEI formation temperature increased the relative amount of Li_2CO_3 to $ROCO_2Li$ (in a solvent of EC, R corresponds to CH_2). Under the higher SEI formation temperature, some metastable complexes in SEI film may transform to stable substances, by the following reaction:

$$2CH_2OCO_2Li + 2e^- + 2Li^+ \rightarrow CH_2CH_2 + 2Li_2CO_3 \quad (10)$$

Thus, it is proposed that the SEI film of group A should contain more insoluble inorganics than that of group C after formation, which made the SEI film of group A more stable than that of group C at the elevated temperature.

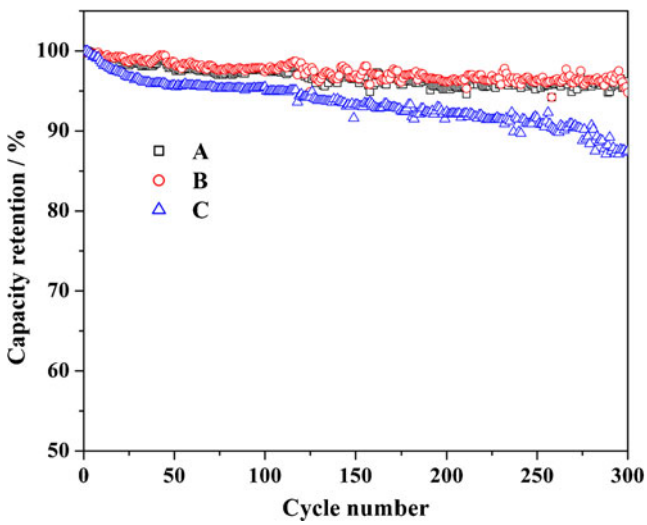

Fig. 9 Cycle performance of Li-ion cells with different formation conditions

Although the SEI formation current density also affected the impedance of SEI film, it played a less significant role in controlling the property of SEI film and the self-discharge capacity loss of the aged cells compared with the SEI formation temperature. Additionally, in the mass production of Li-ion batteries, the formation process is critical because of its economic impact, which is both time- and resource-consuming [29]. It is possible to shorten the formation time by using a higher current density during formation period in the compromise of losing some initial capacity and increasing some irreversible capacity loss during storage. It is noted that the chemistry of SEI film is complicated because the film property is also affected by other factors, such as electrolytes, types of graphite, and surface properties of graphite [1, 24, 30, 31]. Although the results in this work were obtained from only one type of graphite and electrolyte, data from other cells with different types of graphite and electrolyte also indicated that the formation temperature significantly affected the property of SEI layer by changing the SEI compositions [20, 21].

Cycle performance

The capacity loss of a Li-ion cell during cycle is mainly caused by both the cycleable lithium loss resulted from lithium-consuming SEI layer growth and the rate capability loss mostly due to the rise of interfacial resistance [32–35]. Also, the growth of SEI layer can result in an interfacial resistance increase in the cell. Figure 9 shows the cycling performance of the Li-ion cells. After 300 cycles, the capacity retention of group C was 87.5%, about 8% less than that of the other two groups, implying that the higher formation temperature at 45 °C was beneficial to form a stable SEI film to impede capacity fade during cycle. Additionally, the cycling performance of group A and group B was similar, inferring that the formation current density was not a significant factor in controlling the property of the SEI film and the capacity loss of Li-ion cells.

Conclusions

The effect of formation conditions on the aging performance of Li-ion cells during storage and cycle was studied in the three groups of Li-ion cells with various combinations of formation temperatures and current densities. The formation temperature played a significant role in controlling the property of SEI film and the irreversible capacity loss of aged cells. The Li-ion cell formation at 25 °C (group C) suffered greater irreversible capacity loss and had more than 20% increase of the ohmic resistance and the SEI film resistance of the negative electrode than those of the cell formation at 45 °C (group A) after storage at 60 °C for 10 weeks. Both cycle and storage tests implied that a higher formation temperature was contributed to form a stable SEI film on the negative electrode, which can impede the side reaction between the electrode and the electrolyte. However, under the same formation temperature at 45 °C, although the formation current density decreased from 1.077 to 0.043 mA cm^{-2}, it did not significantly affect the capacity loss of the cells either during storage or cycle. Finally, an improvement in the aging performance of Li-ion cells is possible via optimization of formation conditions and/or via selection of suitable materials.

References

1. Verma P, Maire P, Novák P (2010) Electrochim Acta 55:6332–6341
2. Aurbach D, Levi MD, Levi E, Schechter A (1997) J Phys Chem B 101:2195–2206
3. Ohzuku T, Iwakoshi Y, Sawai K (1993) J Electrochem Soc 140:2490–2498
4. Peled E, Golodnitsky D, Ardel G (1997) J Electrochem Soc 144: L208–L210
5. Cheng Y, Wang G, Yan M, Jiang Z (2007) J Solid State Electrochem 11:310–316
6. Park M, Zhang X, Chung M, Less GB, Sastry AM (2010) J Power Sources 195:7904–7929
7. Wang F-M, Cheng H-M, Wu H-C, Chu S-Y, Cheng C-S, Yang C-R (2009) Electrochim Acta 54:3344–3351
8. Park G, Nakamura H, Lee Y, Yoshio M (2009) J Power Sources 189:602–606
9. Zheng M-S, Dong Q-F, Cai H-Q, Jin M-G, Lin Z-G, Sun S-G (2005) J Electrochem Soc 152:A2207–A2210
10. Yamada Y, Iriyama Y, Abe T, Ogumi Z (2009) Langmuir 25:12766–12770
11. Kwak G, Park J, Lee J, Kim S, Jung I (2007) J Power Sources 174:484–492
12. Menkin S, Golodnitsky D, Peled E (2009) Electrochem Commun 11:1789–1791
13. Cho IH, Kim S-S, Shin SC, Choi N-S (2010) Electrochem Solid State Lett 13:A168–A172
14. Yazami R, Reynier YF (2002) Electrochim Acta 47:1217–1223
15. Broussely M, Herreyre S, Biensan P, Kasztejna P, Nechev K, Staniewicz RJ (2001) J Power Sources 97–98:13–21
16. Huang CC, Huang KL, Liu SQ, Zeng YQ, Chen LQ (2009) Electrochim Acta 54:4783–4788
17. Ramasamy RP, White RE, Popov BN (2005) J Power Sources 141:298–306
18. Dolle M, Orsini F, Gozdz AS, Tarascon J-M (2001) J Electrochem Soc 148:A851–A857
19. Zheng T, Gozdz AS, Amatucci GG (1999) J Electrochem Soc 146:4014–4018
20. Lee S-B, Pyun S-I (2002) Carbon 40:2333–2339
21. Lee S-B, Pyun S-I (2003) J Solid State Electrochem 7:201–207
22. Doll M, Grugeon S, Beaudoin B, Dupont L, Tarascon JM (2001) J Power Sources 97–98:104–106
23. Aurbach D (2000) J Power Sources 89:206–218
24. Béuin F, Chevallier F, Vix-Guterl C, Saadallah S, Bertagna V, Rouzaud JN, Frackowiak E (2005) Carbon 43:2160–2167
25. Zhang SS, Xu K, Jow TR (2004) Electrochim Acta 49:1057–1061

26. Ramasamy RP, Lee J-W, Popov BN (2007) J Power Sources 166:266–272
27. Guyomard D, Tarascon JM (1995) J Power Sources 54:92–98
28. Arora P, White RE, Doyle M (1998) J Electrochem Soc 145:3647–3667
29. Lee HH, Wang YY, Wan CC, Yang MH, Wu HC, Shieh DT (2004) J Power Sources 134:118–123
30. Ng SH, Vix-Guterl C, Bernardo P, Tran N, Ufheil J, Buqa H, Dentzer J, Gadiou R, Spahr ME, Goers D, Novák P (2009) Carbon 47:705–712
31. Aurbach D, Talyosef Y, Markovsky B, Markevich E, Zinigrad E, Asraf L, Gnanaraj JS, Kim H-J (2004) Electrochim Acta 50:247–254
32. Ramadass P, Haran B, White R, Popov BN (2002) J Power Sources 112:614–620
33. Kida Y, Kinoshita A, Yanagida K, Funahashi A, Nohma T, Yonezu I (2002) Electrochim Acta 47:4157–4162
34. Safari M, Morcrette M, Teyssot A, Delacourt C (2009) J Electrochem Soc 156:A145–A153
35. Zhang Y, Wang C-Y, Tang X (2010) J Power Sources (in press) doi:10.1016/j.jpowsour.2010.08.070